DUWELL, E. J. & BAENZIGER, N. C. (1955). *Acta Cryst.* **8**, 705.
DUWELL, E. J. & BAENZIGER, N. C. (1960). *Acta Cryst.* **13**, 476.
FITZWATER, D. R., JOHNSTON, T. R., ERBECK, D. H. & RHYNE, M. K. (1964). U.S. Atomic Energy Commission Report IS-954.
GREINER, J. D. (1966). Iowa State Univ., Private communication.
HANSEN, M. & ANDERKO, K. (1958). *Constitution of Binary Alloys*, p. 1008. 2nd ed. New York: McGraw-Hill.
HART, R. R., ROBIN, M. B. & KUEBLER, N. A. (1965). *J. Chem. Phys.* **42**, 3631.
HERSHAFT, A. & CORBETT, J. D. (1963). *Inorg. Chem.* **2**, 979.
HEWAIDY, I. F., BUSMANN, E. & KLEMM, W. (1964). *Z. anorg. allgem. Chem.* **328**, 283.
HULTGREN, R., GINGRICH, N. S. & WARREN, B. E. (1935). *J. Chem. Phys.* **3**, 351.
KETTLE, S. F. A. (1966). *Theoret. Chim. Acta*, **4**, 150.
KJEKSHUS, A. (1964). *Acta Chem. Scand.* **18**, 2379.
LAVES, F. (1956). *Crystal Structure and Atomic Size* in *Theory of Alloy Phases.* Cleveland: Amer. Soc. Metals.
MARSH, R. E. & SHOEMAKER, D. P. (1953). *Acta Cryst.* **6**, 197.
MOORE, C. E. (1958). *Atomic Energy Levels.* Vol. III. Circular No. 467. National Bureau of Standards.
NELSON, J. B. & RILEY, D. P. (1945). *Proc. Phys. Soc. Lond.* **57**, 160.
NIELSEN, J. W. & BAENZIGER, N. C. (1954). *Acta Cryst.* **7**, 277.
PEARSON, W. B. (1964). *Acta Cryst.* **17**, 1.
SCHÄFER, H., JANZON, K. H. & WEISS, A. (1963). *Angew. Chem.* **75**, 451.
SELWOOD, P. W. (1956). *Magnetochemistry*, p. 78. 2nd ed. New York: Interscience.
SILVER, D. (1965). Iowa State Univ., Private communication.
WELLS, A. F. (1950). *Structural Inorganic Chemistry*, p. 455. 2nd ed. London: Oxford Univ. Press.
WILLIAMS, D. E. (1964). U.S. Atomic Energy Commission Report IS-1052.
WILLIAMS, D. E. & RUNDLE, R. E. (1964). *J. Amer. Chem. Soc.* **86**, 1660.
WITTE, J., SCHNERING, H. G. & KLEMM, W. (1964). *Z. anorg. allgem. Chem.* **327**, 260.
ZINTL, E. & DULLENKOPF, W. (1932). *Z. physik. Chem.* **B16**, 195.

Acta Cryst. (1967). **22**, 845

Determination of the Layer Stacking Sequence of a New Complex Mica Polytype: A 4-layer Lithium Fluorophlogopite*

BY HIROSHI TAKEDA†

U.S. Geological Survey, Washington, D.C. 20242, *U.S.A. and The Johns Hopkins University, Baltimore, Maryland, U.S.A.*

(*Received* 6 *July* 1966)

A method of deriving a 'periodic intensity distribution function' that is characteristic of the layer stacking sequence of any mica polytype is given. It is then shown how this function can be directly related to the X-ray diffraction patterns of multi-layer micas so as to establish the particular stacking sequence and thus the structure of the mica polytype. This intensity function is utilized to solve the crystal structure of a newly discovered 4-layer mica polytype, a synthetic lithium fluorophlogopite. This mica is triclinic, space group $C1$, $a=5{\cdot}31$, $b=9{\cdot}19$, $c=40{\cdot}58$ Å, $\alpha=\gamma=90°$, $\beta=100°3'$. The layer stacking sequence of this polytype involves relative layer rotations of 0, 60, 180, and 120°. Atomic parameters for the 80 atoms in the asymmetric unit are given.

Introduction

The principal mica polytypes have been investigated by Hendricks & Jefferson (1939), by Heinrich, Levinson, Levandowski & Hewitt (1953), and more recently by Smith & Yoder (1956), who described the six simplest mica polytypes, namely the $1M$, $2M_1$, $2M_2$, $2O$, $3T$, and $6H$ forms. Zvyagin (1961) gave a method of calculating the structure factors of these simple forms. Sadanaga & Takéuchi (1961) gave an elegant analysis of the possible twin operations found in these polytypes. Burnham & Radoslovich (1964) carefully refined the $2M_1$ muscovite structure.

Ross & Wones (1965) and Takeda & Donnay (1965) have found many more complex polytypes not included among those previously described. Two of these newly discovered polytypes have 4-layer structures. A method of generating all possible structure models for mica polytypes with a given layer repeat has been developed by Ross, Takeda & Wones (1966). Some of the simpler

---

* Publication authorized by the Director, U.S. Geological Survey. Work was, in part, carried out at the Crystallographic Laboratory, The Johns Hopkins University, Baltimore, Md. under National Science Foundation Grant GP 1565.

† Present address, Mineralogical Institute, The University of Tokyo, Hongo, Tokyo, Japan.

models can be identified by unit-cell parameters, symmetry, and rules for 'structural extinctions'. Many models, however, cannot be so identified; thus it is necessary to find a method of systematically analyzing the X-ray intensities in order positively to identify the polytype.

Sadanaga & Takeda (1964) and Takeda (1961) have used a periodic intensity distribution function to determine the structure of the complex sulfo-salt, zinkenite ($PbS.Sb_2S_3$). A function similar to this is developed in this paper for analysis of the various stacking sequences in micas. The function is then applied to the solution of the stacking sequence of a new 4-layer triclinic lithium fluorophlogopite.

Mica polytypism

The features of mica structures critical to the understanding of polytypism are described by Hendricks & Jefferson (1939), Smith & Yoder (1956), and Zvyagin (1962). The single mica layer consists of three portions: a sheet of octahedrally coordinated cations sandwiched between two identical sheets of linked $(Si,Al)O_4$ tetrahedra. Between these composite mica layers lie the interlayer cations.

Polytypism occurs in micas because the surface oxygen atoms of the tetrahedral layer possess pseudo-hexagonal or pseudo-trigonal symmetry, thus permitting the single monoclinic mica layer to superimpose on an adjacent layer in six possible orientations involving relative layer rotations of 0, ± 60, ± 120, or 180°; the rotation axis passes through the interlayer potassium atom and is perpendicular to the plane of the surface atoms (parallel to **c***). Mica polytypism is thus accounted for by arranging N layers in a particular rotational sequence, the sequence repeating after every Nth layer.

In the simple $1M$ and $2M_1$ mica structures thus far studied the symmetry of the surface oxygen layers is distorted from the ideal hexagonal motif to a trigonal one, causing the coordination polyhedron about the interlayer potassium atom to change from a regular hexagonal prism (12-fold coordination) to a trigonal antiprism (6-fold coordination).

For multi-layer mica polytypes in which the symmetry of the surface oxygen layers is trigonal the potassium coordination polyhedron remains in the form of a trigonal antiprism if the relative rotation of adjacent layers is 0, 120, or 240°. However, if the relative rotation of adjacent mica layers is 60, 180, or 300° the coordination polyhedron about potassium becomes a trigonal prism.

For the purposes of this paper the six possible orientations of the single mica layer will be designated A, B, C, $\bar{A}$, $\bar{B}$, and $\bar{C}$ in accordance with Zvyagin's (1961) notation. Each of these orientations is defined by an angle of rotation about **c*** (Table 1 and Fig. 1) of a single mica layer with respect to a *standard* layer in the Zvyagin C setting. The *standard* mica layer is defined as having the 1-layer monoclinic axial setting, space group $C2/m$, with $a\sqrt{3}=b$, $c \cos \beta^* = a/3$, $\beta = 100°$, and oriented as shown in Fig. 1.

The stacking sequence of the N-layer mica is expressed with a series of N letters, the nth letter of the series referring to the Zvyagin orientation of the nth mica layer as depicted in Fig. 1. This series of letters expressing the stacking sequence is referred to as the *Zvyagin oriented stacking symbol.* The *vector stacking symbols* (Table 2) of Ross, Takeda & Wones (1966) give the *relative* rotations between adjacent layers and are useful in generating all the possible mica polytypes with a given layer repeat. Only the Zvyagin symbols will be used in this paper.

Each individual layer of the N-layer polytype displaces the structure parallel to the (001) plane. This displacement by each layer is expressed in terms of the components x^L and y^L directed parallel to the a and b axes of the N-layer mica. The a and b axial direc-

Table 1. *Coordinate transformation* $T_n = t_{11}t_{12}/t_{21}t_{22}$, *layer displacements* (x^L, y^L), *and origin displacement* (x^o, y^o), *for the six possible Zvyagin orientations of the single mica layer*

Twin axis	Rotation about **c***	Layer type	$\begin{pmatrix} t_{11} & t_{12} \\ t_{21} & t_{22} \end{pmatrix}$	$\begin{pmatrix} x^L \\ y^L \end{pmatrix}$	$\begin{pmatrix} x^0 \\ y^0 \end{pmatrix}$ †
	0°	C*	$\begin{pmatrix} 1 & 0 \\ 0 & 1 \end{pmatrix}$	$\begin{pmatrix} -\frac{1}{3} \\ 0 \end{pmatrix}$	$\begin{pmatrix} 0 \\ 0 \end{pmatrix}$
[110]	60	$\bar{B}$	$\begin{pmatrix} \frac{1}{2} & -\frac{3}{2} \\ \frac{1}{2} & \frac{1}{2} \end{pmatrix}$	$\begin{pmatrix} \frac{1}{3} \\ \frac{1}{3} \end{pmatrix}$	$\begin{pmatrix} \frac{3}{4} \\ \frac{1}{4} \end{pmatrix}$
[310]	120	A	$\begin{pmatrix} -\frac{1}{2} & -\frac{3}{2} \\ \frac{1}{2} & -\frac{1}{2} \end{pmatrix}$	$\begin{pmatrix} -\frac{1}{3} \\ \frac{1}{3} \end{pmatrix}$	$\begin{pmatrix} \frac{5}{4} \\ \frac{1}{4} \end{pmatrix}$
[100]	180	$\bar{C}$	$\begin{pmatrix} -1 & 0 \\ 0 & -1 \end{pmatrix}$	$\begin{pmatrix} \frac{1}{3} \\ 0 \end{pmatrix}$	$\begin{pmatrix} 1 \\ 1 \end{pmatrix}$
[3$\bar{1}$0]	−120	B	$\begin{pmatrix} -\frac{1}{2} & \frac{3}{2} \\ -\frac{1}{2} & -\frac{1}{2} \end{pmatrix}$	$\begin{pmatrix} -\frac{1}{3} \\ -\frac{1}{3} \end{pmatrix}$	$\begin{pmatrix} \frac{1}{4} \\ \frac{3}{4} \end{pmatrix}$
[1$\bar{1}$0]	−60	$\bar{A}$	$\begin{pmatrix} \frac{1}{2} & \frac{3}{2} \\ -\frac{1}{2} & \frac{1}{2} \end{pmatrix}$	$\begin{pmatrix} \frac{1}{3} \\ -\frac{1}{3} \end{pmatrix}$	$\begin{pmatrix} -\frac{1}{4} \\ \frac{3}{4} \end{pmatrix}$

* Standard setting. † Potassium atom at $(0,\frac{1}{2},0)$.

tions are chosen so as to lie parallel to the a and b axes of the *standard* layer. The total displacement is the sum of the individual displacement vectors of the N different layers which make up the stacking sequence. The individual displacement vectors for the single mica layer in the six possible Zvyagin orientations are given in Table 1. Here it is seen that the values of x^{L} and y^{L} are either $\pm\frac{1}{3}$ or 0. Also, the sum of the vectors x^{L} and y^{L} for N-layers, after subtraction of an integer, is either (0,0), ($\pm\frac{1}{3}$,0), or (0, $\pm\frac{1}{3}$). These three 'sets' of 'total displacement vectors' symbolized by 'Δt' define the three possible axial settings for the N-layer mica, *i.e.*,

(1) $\Delta t=(0,0)$, $\alpha=\beta=\gamma=90°$, metrically orthorhombic, $2O$ type axial setting,

(2) $\Delta t=(\pm\frac{1}{3},0)$, $\alpha=\gamma=90°$, $\beta>90°$, metrically monoclinic, b unique, $1M$ type axial setting, and

(3) $\Delta t=(0,\pm\frac{1}{3})$, $\beta=\gamma=90°$, $\alpha>90°$, metrically monoclinic, a unique, $2M_2$ type axial setting.

The axial lengths of micas in any of the above settings are $a\sqrt{3}=b\simeq 9$ Å and $c \sin\alpha^* \sin\beta^* \simeq 10N$ Å.

Theory

Consider the case in which there are two identical structural units (say two molecules) in the same orientation separated by a vector $\mathbf{t}$. The composite Fourier transform G^c is given (Lipson & Taylor, 1958, p. 11) as

$$G^c(\mathbf{h}) = G(\mathbf{h})(1+\exp 2\pi i\mathbf{t}\,.\,\mathbf{h}) \qquad (1)$$

where G is the Fourier transform of the single molecule. The expression $(1+\exp 2\pi i\mathbf{t}\,.\,\mathbf{h})$ is a *fringe* function which is a periodic function characterized by the vector $\mathbf{t}$. One cannot generally observe this periodicity directly in the X-ray diffraction pattern for the intensity distribution is modified by G, the transform of the single unit. Also, for triperiodic structures this function can only be analyzed at the reciprocal lattice nodes of the unit cell.

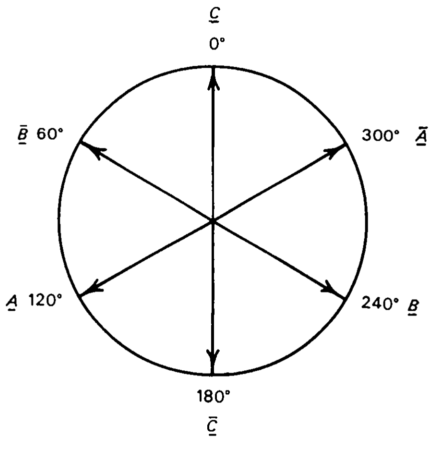

Fig. 1. Designation of the six Zvyagin *oriented stacking symbols*. Arrows indicate the mirror plane and direction of the layer stagger of the individual $C2/m$ layer (as used by Smith & Yoder, 1956, p. 213) in its six possible orientations A, B, C, $\bar{A}$, $\bar{B}$, and $\bar{C}$. The orientation of the *standard* mica layer is C with $\mathbf{a}$ directed down, $\mathbf{b}$ to the right of the figure, and $\mathbf{c}^*$ towards the reader's eye. The β angle is 100°.

In the case of mica polytypes G is replaced by the Fourier transform of the single mica layer, and the vector $\mathbf{t}$ becomes a 'stacking' vector describing the translational and rotational relations between adjacent mica layers. In the following, the Fourier transform of a mica structure composed of N-layers will be examined and a method developed for eliminating the effect of intensity modulation by the Fourier transform of the single layer. An expression will be derived which reflects the Fourier transform of only the rotational and translational distribution of the mica layers, a periodic 'fringe function'. It will then be shown how this expression can be directly related to the X-ray diffraction pattern so as to describe positively the stacking sequence of any mica polytype.

Consider an N-layer mica polytype having the $1M$ type axial setting with $a\sqrt{3}=b$, $\alpha=\gamma=90°$, $\beta=100°$ and with the axes directed the same as those of the *standard* layer of Fig. 1. The atomic coordinates of the nth layer (x_n, y_n, z_n) in the sequence of N layers must be derived in terms of the atomic coordinates (x,y,z) of the *standard* layer. If the transformation matrix (Table 1) for a rotation about $\mathbf{c}^*$ of the nth layer is

$$T_n = t_{11}t_{12}/t_{21}t_{22} \qquad (2)$$

then the atomic coordinates for the nth layer are expressed, in fractions of the cell edges of the *standard* layer, as follows:

$$x_n = t_{11}(x-z/3)+t_{12}y+x_n^o+\sum_{i=1}^{n-1} x_i^L+(z+n-1)/3, \qquad (3)$$

$$y_n = t_{21}(x-z/3)+t_{22}y+y_n^o+\sum_{i=1}^{n-1} y_i^L\,, \qquad (4)$$

$$z_n = z+(n-1)\,, \qquad (5)$$

where n is any particular layer in a sequence of N layers, x_n^o and y_n^o give the origin displacement which will bring the lower rings of surface oxygen atoms of the nth layer on top of the upper oxygen rings of the $(n-1)$th layer after rotation, and x_i^L and y_i^L give the layer displacement along the a and b axes, respectively, of the ith layer. The values T_n, x^{L}, y^{L}, x^{o} and y^{o} for the six possible Zvyagin orientations of the mica layer are given in Table 1.

The rotational and translational transformations are accomplished in the orthogonal coordinate system abc^* where a, b, and c^* are the axes of the *standard* mica layer. The x coordinates of the *standard* layer are first transformed into the orthogonal coordinates x_0 with the relation

$$x_0 = x-(c/a)\cos\beta^*\,.\,z = x-(z/3)\,.$$

Then, after the transformation from x_0 to x_o' (3), x_o' is transformed back into the original *standard* layer coordinate system abc using the relation

$$x_n = x_o' + (z_n/3)\,.$$

In the above derivations, the unit-cell edges of the *standard* mica layer have been retained. Thus, the values of z_n (5) are always greater than one except for those atoms within the 1st layer. If the atomic coordinates x_n, y_n, and z_n are related to the unit cell of the N-layer mica, the value of x_n and y_n will remain the same but the value z_n will be given by

$$z_n = z/N + (n-1)/N\,. \tag{6}$$

Generation of atomic coordinates for mica polytypes with $2O$ and $2M_2$ type axial settings is easily accomplished by using relations slightly modified from (3), (4), and (5).

From the values of the atomic coordinates x_n, y_n, and z_n, the Fourier transform of the nth layer is given as

$$G_n(hkl) = \sum_j f_j \exp[2\pi i(hx_{nj} + ky_{nj} + lz_{nj})]\,, \tag{7}$$

or

$$G_n(hkl) = G(h'k'l') \exp[2\pi i(h\Delta x_n + k\Delta y_n + ln - l)]\,, \tag{8}$$

where

$$G(h'k'l') = \sum_j f_j \exp[2\pi i(h'x_j + k'y_j + l'z_j)]\,, \tag{9}$$

$$h' = t_{11}h + t_{21}k\,, \tag{10}$$

$$k' = t_{12}h + t_{22}k\,, \tag{11}$$

$$l' = l + [(1-t_{11})h - t_{21}k]/3 \tag{12}$$

$$\Delta x_n = x_n^o + (n-1)/3 + \sum_{i=1}^{n-1} x_i^L \tag{13}$$

and

$$\Delta y_n = y_n^o + \sum_{i=1}^{n-1} y_i^L\,. \tag{14}$$

$G_n(hkl)$ consists of the product of two terms:

(1) the Fourier transform of the single mica layer $G(h'k'l')$ which is index transformed (10, 11, 12) in accordance with the rotation about $\mathbf{c}^*$ of the layer in direct space (Table 1) and (2) the exponential term, a periodic function analogous to the 'fringe function', which includes the components of the displacement vector, Δx_n and Δy_n (13, 14).

Finally, the Fourier transform for the entire N-layer structure is expressed as the sum of the transforms of all the individual layers, *i.e.*,

$$G^N(hkl) = \sum_{n=1}^{N} G_n(hkl)\,. \tag{15}$$

In order to compare the intensity distribution calculated from the Fourier transform with the intensity distribution observed in the X-ray photographs, reflections should be chosen that are especially sensitive to the stacking sequences. Experience shows that the reciprocal lattice rows $02l$, $04l$, $11l$, $22l$, $\bar{1}1l$, $\bar{2}2l$, $20l$, $13l$, and $\bar{1}3l$ are the most useful for distinguishing the stacking sequences in micas. As an example, let us examine the periodic intensity distribution along the $02l$ reciprocal lattice row for a 4-layer mica with the stacking sequence $C\acute{A}\bar{C}\bar{B}$. The Fourier transform $G^4(02l)$ is given as

$$\begin{aligned} G^4(02l) = {} & G(02l) + G(1\,.\,1\,.\,\bar{l}-\tfrac{1}{3}) \exp[2\pi i(\tfrac{3}{2}+l)] \\ & + G(02l) \exp[2\pi i(\tfrac{4}{3}+2l)] \\ & + G(1\,.\,1\,.\,l-\tfrac{1}{3}) \exp[2\pi i(-\tfrac{1}{6}+3l)]\,, \end{aligned} \tag{16}$$

where $G(02l)$, $G(1\,.\,1\,.\,l-\tfrac{1}{3})$, and $G(1\,.\,1\,.\,\bar{l}-\tfrac{1}{3})$ are the Fourier transforms of the single mica layer index transformed in accordance with the rotation of each particular layer of the 4-layer series.

Because of the special nature of the mica structure the value of the transform $G(1\,.\,1\,.\,l-\tfrac{1}{3})$ is almost exactly identical with $-G(02l)$ as is shown in Fig. 2. With the assumption that it is rigorously identical (16) can be written as

$$\begin{aligned} G^4(02l) = {} & G(02l)\{1 - \exp[2\pi i(\tfrac{3}{2}+l)] \\ & + \exp[2\pi i(\tfrac{4}{3}+2l)] - \exp[2\pi i(-\tfrac{1}{6}+3l)]\}\,. \end{aligned} \tag{17}$$

Equation (17) now consists only of a factor $G(02l)$ and an exponential term. If a function $S^N(02l)$ is now defined,

$$S^N(02l) \equiv G^N(02l)/G(02l)\,, \tag{18}$$

the effect of the Fourier transform of the single mica layer is removed leaving only an exponential term – the fringe function. This function is periodic, the values of S^N repeating along reciprocal lattice row lines parallel to $\mathbf{c}^*$ with the same period as that of the reciprocal lattice of the 1-layer monoclinic ($1M$) mica.

If the Miller indices of the N-layer mica (hkL) are now introduced, the periodicity of this function, $S^N(hkL)$, is described as repeating along reciprocal lattice rows parallel to $\mathbf{c}^*$ after every Nth reciprocal lattice node of the N-layer lattice. The repeating set of N characteristic S^N terms is designated the *periodic intensity distribution function,*

$$\overline{S^N}(hk\hat{L})\,,$$

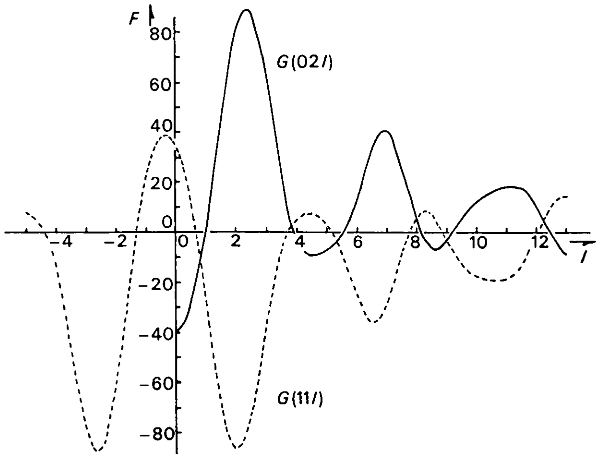

Fig. 2. Fourier transform of the 1-layer monoclinic lithium fluorophlogopite along the reciprocal lattice rows 02*l* and 11*l*. The transform was calculated from the unit-cell parameters, atomic positions, and chemical composition given by Takeda & Donnay (1966).

where $\hat{L}=0,1,2\ldots(N-1)$. The S^N terms have the same value for all reflections which obey the relation $L=\hat{L}$ mod N for fixed h and k. By evaluating $\overline{S^N}(hk\hat{L})$ along two or three row lines parallel to **c*** the stacking sequence and hence the mica polytype may be positively identified. In practice it has been found that the calculation of the periodic intensity distribution along three of the following reciprocal lattice rows is usually sufficient to identify the stacking sequence: $02L$, $11L$, $\bar{1}1L$, and $20L$. Lattice rows $04L$, $22L$, $\bar{2}2L$, $13L$, and $\bar{1}3L$ can be used equally well for identification of the stacking sequence. Equations similar to (17) are easily developed for calculating the periodic intensity distribution along any reciprocal lattice rows parallel to **c***. In the last section of this paper the method of determining the stacking sequence of a 4-layer mica is given.

An observed value of $S_o^N(hkL)$ is defined as

$$|S_o^N(hkL)| \equiv |F_o^N(hkL)|/|G(hkl)| , \tag{19}$$

where $|F_o^N(hkL)|$ is an observed structure factor of an N-layer mica, L being referred to the N-layer unit cell. $G(hkl)$ is the Fourier transform of a single mica layer, l referring to the third Miller index of the 1-layer ($1M$) mica. This transform is evaluated at the same point in reciprocal space as the observed structure factor. For multi-layer mica polytypes having the $1M$ setting, $\beta=100°$ (Table 2), the relation between the Miller index L of the N-layer cell and the index l of the single layer transform is

$$l=L/N . \tag{20}$$

Table 2. *The* 14 *polytypes which have the* 1*M type axial setting**, *of the* 26 *possible* 4-*layer polytypes* (*after Ross, Takeda & Wones*, 1966)

Vector stacking symbols†	Zvyagin oriented stacking symbols
$4M_1$ $[020\bar{2}]$	$AABB$
$4M_2$ $[2220]$	$CABC$
$4M_3$ $[2\bar{2}\bar{2}2]$	$CACB$
$4M_4$ $[0033]$	$\bar{C}\bar{C}\bar{C}C$
$4M_5$ $[1122]$	$C\bar{A}\bar{C}\bar{B}$
$4Tc_1$ $[2\bar{2}33]$	$\bar{A}A\bar{A}\bar{B}$
$4Tc_2$ $[1\bar{1}\bar{2}2]$	$\bar{C}\bar{A}\bar{C}A$
$4Tc_3$ $[13\bar{2}\bar{2}]$	$C\bar{C}\bar{A}\bar{B}$
$4Tc_4$ $[0213]$	$A\bar{A}\bar{A}\bar{B}$
$4Tc_5$ $[0132]$	$\bar{C}\bar{C}\bar{A}A$
$4Tc_8$ $[002\bar{2}]$	$BBBC$
$4Tc_9$ $[\bar{1}1\bar{2}2]$	$\bar{A}B\bar{A}\bar{C}$
$4Tc_{10}$ $[001\bar{1}]$	$\bar{A}\bar{A}\bar{A}C$
$4Tc_{11}$ $[011\bar{2}]$	$\bar{B}\bar{B}A\bar{C}$

* Mica polytypes with the $1M$ type axial setting have the following unit-cell dimensions: $a\sqrt{3}=b\simeq 9{\cdot}2$ Å, $c \sin\beta^* \simeq 10N$ Å, $\alpha=\gamma=90°$, and $\beta\simeq 100°$.

† M = monoclinic, Tc = triclinic.

The values of $|\overline{S_o^N}(hkL)|$ may not show the exact periodicity predicted, owing to errors in measurement of F_o and errors in evaluating $G(hkl)$. In order to average out the error within any particular set of $|\overline{S_o^N}|$ values it is useful to measure over several repeats within one reciprocal lattice row. Also, measurement of intensities at the point where the value of $G(hkl)$ approaches zero should be avoided. To obtain the values of $G(hkl)$ the structure and composition of the 1-layer mica polytype should be approximately known.

In understanding the meaning of $\overline{S^N}$ in direct space, it should be noted that, even though we are dealing with translation and rotation of the layers, both operations can be treated as if only translation occurs by introduction of the relation

$$G(1\,.\,1\,.\,l-\tfrac{1}{3})=-G(02l)\,.$$

The relation actually eliminates the effect of rotation from G^N, and implies that every 60° rotation of a layer about **c*** changes the sign of G^N but not the magnitude. Thus, one can express S^N of a reciprocal lattice row parallel to **c*** as a function of l and components of translational vectors, for fixed h and k.

The periodic intensity distribution function $\overline{S^N}$ may be related to direct space by the following: the Fourier transform of the N-layer mica is expressed as†

$$G^N(\mathbf{l})=G(\mathbf{l})\times\{\overline{S^N}(\hat{L})*\Delta(\mathbf{l})\}\ ,$$

where $*$ stands for the convolution of two functions and × for the product, and $\Delta(\mathbf{l})$ for a peak function expressing the reciprocal lattice repeat along **c*** of the single mica layer. The Fourier transform of $G^N(\mathbf{l})$ gives the electron density function of the N-layer mica,

$$\varrho^N(\mathbf{z})=\varrho(\mathbf{z})*\{\overline{s^N}(\hat{Z})\times\delta(\mathbf{z})\}\ ,$$

where $\varrho(\mathbf{z})$ is the electron density function of a 1-layer mica in the standard C orientation, $\delta(\mathbf{z})$ is a peak function which expresses the lattice translation, and $\overline{s^N}(\hat{Z})$ is the transform of $\overline{S^N}(\hat{L})$. The function $\overline{s^N}(\hat{Z})$ modifies the unit-cell translation of the 1-layer mica with the period of the N-layer polytype, and thus describes the stacking sequence. Therefore, $\overline{S^N}(\hat{L})$, the transform of $\overline{s^N}(\hat{Z})$, contains the optimum information on the nature of the stacking sequence.

Experimental

A sample of lithium fluorophlogopite,

$$K_{0{\cdot}86}(Mg_{2{\cdot}26}Li_{0{\cdot}54}Al_{0{\cdot}08})(Si_{3{\cdot}83}Al_{0{\cdot}17})O_{10}F_2,$$

synthesized by the Mycalex Corporation of America, was provided by Dr H. S. Yoder, Jr. The sample is composed mainly of the 1-layer monoclinic mica polytype ($1M$), for which the structure has been reported (Takeda & Donnay, 1966). Also found in this sample was a four-layer triclinic polytype the structure of which is described here.

This crystal was first mounted along the b axis, and non-integrated Weissenberg photographs ($k=0$ to 6) were taken with Cu $K\alpha$ radiation. The crystal was then mounted about **c*** and the following reciprocal lattice nets were photographed with the precession camera

---

† G^N, G, S^N, and Δ are of course functions of all three Miller indices, and ϱ^N, ϱ, s^N, and δ are functions of all three spatial coordinates, but it is the dependence on **l** and **z** respectively that we wish to emphasize here.

using Mo $K\alpha$ radiation: $0kL$, hhL, $\bar{h}hL$, $h0L$, $h3hL$, and $\bar{h}3hL$. Upper level photographs of these zones were also obtained.

The intensities of the $00L$, $02L$, $11L$, $\bar{1}1L$, and $20L$ reflections were measured with the aid of a calibrated intensity scale, and then Lorentz–polarization corrections for the Weissenberg photographs were applied.

Unit cell and space group

The reduced cell dimensions, obtained from the precession photographs, are: $a=5{\cdot}31$, $b=9{\cdot}19$, $c=40{\cdot}0$ Å, $\alpha=\gamma=90°$, and $\beta=92°35'$. The diffraction aspect is C^*. A non-reduced cell may be chosen with $\beta=100°3'$ and $c=40{\cdot}58$ Å, the other parameters remaining the same. This cell, which is more convenient to use for the structure determination, has the following presence criteria in addition to that of the C lattice: when both h and $k=0$ mod 3, $L=0$ mod 4. The symmetry of the intensity distribution shown by the $0kL$ precession photograph is $l2$. The upper level a-axis precession photographs do not show any lines of symmetry†; thus the crystal is triclinic. If only zero-level $h0L$, $0kL$, and $hk0$ photographs of this mica were examined, one would assume this structure to be monoclinic. The space group as deduced from the stacking sequence is $C1$.

The structure determination

There are twenty-six possible mica polytypes having a 4-layer structure (Ross, Takeda & Wones, 1966). These may be divided, as discussed previously, into three groups according to their total layer displacement Δt: the $2O$, the $1M$, and the $2M_2$ types. The 4-layer polytypes found to date belong to the second group with $1M$ type settings for which a non-reduced axial setting with $\beta=100°$ can be chosen. The structure of this mica will be described in terms of this setting.

Fourteen of the twenty-six 4-layer polytypes belong to the group with $1M$ type settings and are listed in Table 2 with both the vector stacking symbols of Ross, Takeda & Wones (1966) and the oriented symbols of Zvyagin (1961). Of these fourteen models five are monoclinic and nine are triclinic. Five of the nine triclinic polytypes, $4Tc_1$, $4Tc_2$, $4Tc_3$, $4Tc_4$, and $4Tc_5$ have the same unit-cell parameters and pseudo-monoclinic symmetry as for lithium fluormica (Ross, Takeda & Wones, 1966). All these structures give diffraction pat-

Table 4. *Atomic parameters**
of the 4-layer lithium fluoro-phlogopite

Atom†	x	y	z	B(Å)²	Atom†	x	y	z	B(Å)²
(K)11	0.0000	0.5000	0.0000	2.13	(K)31	0.3333	0.5000	0.5000	2.13
(O1)11	0.5874	0.5000	0.0416	1.42	(O1)31	0.5221	0.2660	0.5416	1.42
(O1)12	0.0792	0.5000	0.2084	1.42	(O1)32	0.7105	0.4007	0.7084	1.42
(O2)11	0.2895	0.2654	0.0417	1.30	(O2)31	0.1240	0.2342	0.5417	1.30
(O2)14	0.8771	0.2346	0.2082	1.30	(O2)34	0.2094	0.4324	0.7082	1.30
(O2)13	0.7895	0.2346	0.0417	1.30	(O2)33	0.9702	0.4996	0.5417	1.30
(O2)12	0.3771	0.2654	0.2082	1.30	(O2)32	0.4132	0.1670	0.7082	1.30
(SIAL)11	0.5747	0.3335	0.0562	0.70	(SIAL)31	0.9082	0.3331	0.5562	0.70
(SIAL)14	0.5920	0.1665	0.1937	0.70	(SIAL)34	0.4251	0.3336	0.6937	0.70
(SIAL)13	0.0747	0.1665	0.0562	0.70	(SIAL)33	0.4017	0.1666	0.5562	0.70
(SIAL)12	0.0920	0.3335	0.1937	0.70	(SIAL)32	0.4246	0.0001	0.6937	0.70
(O3)11	0.6302	0.3335	0.0977	0.85	(O3)31	0.9635	0.3332	0.5977	0.85
(O3)14	0.5365	0.1665	0.1522	0.85	(O3)34	0.3698	0.3335	0.6522	0.85
(O3)13	0.1302	0.1665	0.0977	0.85	(O3)33	0.4640	0.1667	0.5977	0.85
(O3)12	0.0365	0.3335	0.1522	0.85	(O3)32	0.8693	0.5000	0.6522	0.85
(F)11	0.1351	0.5000	0.1005	1.10	(F)31	0.9668	0.0005	0.6005	1.10
(F)12	0.5316	0.5000	0.1495	1.10	(F)32	0.3665	0.1661	0.6495	1.10
(MGLIM)11	0.8333	0.5000	0.1250	0.53	(MGLIM)31	0.6667	0.3333	0.6250	0.53
(MGLI)11	0.8333	0.1692	0.1250	0.55	(MGLI)31	0.1629	0.4987	0.6250	0.55
(MGLI)12	0.3333	0.3308	0.1250	0.55	(MGLI)32	0.1705	0.1679	0.6250	0.55
(K)21	0.6667	0.5000	0.2500	2.13	(K)41	0.0000	0.1667	0.7500	2.13
(O1)21	0.2541	0.5000	0.2916	1.42	(O1)41	0.8214	0.4007	0.7916	1.42
(O1)22	0.7459	0.5000	0.4584	1.42	(O1)42	0.1785	0.2660	0.9584	1.42
(O2)21	0.9562	0.2654	0.2917	1.30	(O2)41	0.3207	0.4324	0.7917	1.30
(O2)24	0.5438	0.2346	0.4582	1.30	(O2)44	0.6793	0.2342	0.9582	1.30
(O2)23	0.4562	0.2346	0.2917	1.30	(O2)43	0.5245	0.1670	0.7917	1.30
(O2)22	0.0438	0.2654	0.4582	1.30	(O2)42	0.4755	0.4996	0.9582	1.30
(SIAL)21	0.2414	0.3335	0.3062	0.70	(SIAL)41	0.5751	0.3336	0.8062	0.70
(SIAL)24	0.2586	0.1665	0.4437	0.70	(SIAL)44	0.4249	0.3331	0.9437	0.70
(SIAL)23	0.7414	0.1665	0.3062	0.70	(SIAL)43	0.5746	0.0001	0.8062	0.70
(SIAL)22	0.7586	0.3335	0.4437	0.70	(SIAL)42	0.9254	0.1666	0.9437	0.70
(O3)21	0.2968	0.3335	0.3477	0.85	(O3)41	0.6305	0.3335	0.8477	0.85
(O3)24	0.2032	0.1665	0.4022	0.85	(O3)44	0.3695	0.3332	0.9022	0.85
(O3)23	0.7968	0.1665	0.3477	0.85	(O3)43	0.6300	0.0000	0.8477	0.85
(O3)22	0.7032	0.3335	0.4022	0.85	(O3)42	0.8700	0.1667	0.9022	0.85
(F)21	0.8018	0.5000	0.3505	1.10	(F)41	0.1345	0.1661	0.8505	1.10
(F)22	0.1982	0.5000	0.3995	1.10	(F)42	0.3654	0.0006	0.8995	1.10
(MGLIM)21	0.5000	0.5000	0.3750	0.53	(MGLIM)41	0.0000	0.3333	0.8750	0.53
(MGLI)21	0.5000	0.1692	0.3750	0.55	(MGLI)41	0.5038	0.1679	0.8750	0.55
(MGLI)22	0.0000	0.3308	0.3750	0.55	(MGLI)42	0.4962	0.4987	0.8750	0.55

* Calculated with the use of the following unit-cell parameters: space group $C1$, $a=5{\cdot}31$, $b=9{\cdot}19$, $c=40{\cdot}58$ Å, $\alpha=\gamma=90°0'$, and $\beta=100°3'$.

† Atomic designations are as follows: (K) potassium; (O1), (O2), (O3) oxygen; (SIAL) silicon and aluminum; (F) fluorine; (MGLIM), (MGLI) magnesium and lithium. The first number to the right of the atomic designation gives the number of the layer (1, 2, 3, or 4) in which the atom lies. The next number to the right is the atomic site designation. Atomic positions and temperature factors are derived from those of the refined $1M$ lithium fluorophlogopite (Takeda & Donnay, 1966).

Table 3. *Calculated and observed periodic intensity distribution functions,* $\overline{S^4}(02\hat{L})$, $\overline{S^4}(11\hat{L})$, *and* $\overline{S^4}(\bar{1}1\hat{L})$ *for the* $4Tc_1$, $4Tc_2$, $4Tc_3$, $4Tc_4$, *and* $4Tc_5$ *polytypes*

			Calculated				
	$\hat{L}$	Observed	$4Tc_5$	$4Tc_4$	$4Tc_3$	$4Tc_2$	$4Tc_1$
$02\hat{L}$	0	2·79	2·646	1·000	2·646	2·000	2·000
	1	1·91	1·732	1·732	1·732	2·450	0
	2	1·60	1·732	3·000	1·732	0	3·464
	3	1·69	1·732	1·732	1·732	2·450	0
$11\hat{L}$	0	1·20	1·000	2·646	2·000	2·000	2·000
	1	1·69	1·732	1·732	2·450	0	2·450
	2	2·49	3·000	1·732	0	3·464	0
	3	1·62	1·732	1·732	2·450	0	2·450
$\bar{1}1\hat{L}$	0	1·15	1·000	1·000	2·646	1·000	1·000
	1	0·84	0·897	0·897	1·732	0·897	0·897
	2	1·69	1·732	1·732	1·732	1·732	1·732
	3	3·10	3·346	3·346	1·732	3·346	3·346

---

† Only those reflections with $k=0$ mod 3 show one symmetry line perpendicular to **b***.

terns which possess $l/2$ symmetry in the b^*c^* plane. A 'periodic intensity distribution function' was calculated for each of these five models using a FORTRAN-II program (PLYTP) written for the IBM 7094 computer.

The observed values of the intensity function $\overline{S_o^N}(hk\hat{L})$ were obtained by means of equation (19). Ten measurements for each value of $\hat{L}$ were made and averaged. The resulting average observed S_o^N values are given in Table 3 and are compared with the calculated S_c^N values of the $4Tc_1$, $4Tc_2$, $4Tc_3$, $4Tc_4$, and $4Tc_5$ polytypes for the $02\hat{L}$, $11\hat{L}$, and $\bar{1}1\hat{L}$ reflections. The Fourier transform of the *standard* mica layer, $G(hkl)$, was computed with the use of atomic coordinates and temperature factors of the $1M$ lithium fluormica reported by Takeda & Donnay (1966). The computation was carried out by the structure factor calculation subroutine of the least-squares refinement program of Busing, Martin & Levy (1962) as modified by the present author. The observed structure factors of the 4-layer lithium fluormica were scaled using the $00L$ reflections as a standard.

Table 5. *Observed and calculated structure factors of the* $4Tc_5$ *triclinic lithium fluorophlogopite*

The calculated structure factors are obtained by using the atomic parameters given in Table 4.

H	K	L	FO	FC	A	B
0	0	1	0.0	0.	0.	0.
0	0	2	0.0	0.	0.	0.
0	0	3	0.0	0.	0.	0.
0	0	4	124.12	160.77	-160.77	0.24
0	0	5	0.0	0.00	0.00	0.
0	0	6	0.0	0.00	0.00	0.
0	0	7	0.0	0.00	0.00	0.
0	0	8	77.15	70.49	-70.49	0.81
0	0	9	0.0	0.	0.	0.
0	0	10	0.0	0.	0.	0.
0	0	11	0.0	0.00	0.00	0.
0	0	12	295.73	417.73	-417.73	0.86
0	0	13	0.0	0.	0.	0.
0	0	14	0.0	0.00	0.00	0.
0	0	15	0.0	0.	0.	0.
0	0	16	157.39	155.62	155.62	0.43
0	0	20	372.38	436.50	436.49	-2.48
0	0	24	169.68	130.07	130.07	0.75
0	0	28	240.16	200.39	-200.39	1.18
0	0	32	292.46	254.01	254.01	-0.85
0	0	36	136.26	82.37	-82.37	-0.32
0	2	3	13.93	19.20	11.23	15.57
0	2	4	20.15	16.77	16.37	3.65
0	2	5	39.12	48.36	22.33	42.89
0	2	6	60.79	85.80	74.27	-42.96
0	2	7	93.19	120.04	-61.61	-103.02
0	2	8	152.52	223.54	210.88	74.15
0	2	9	118.61	158.26	80.29	136.38
0	2	10	122.85	155.76	134.83	-77.99
0	2	11	117.01	139.21	-68.80	-121.02
0	2	12	155.84	168.70	159.92	53.73
0	2	13	77.59	78.40	38.13	68.50
0	2	14	48.46	45.77	39.62	-22.92
0	2	15	24.76	19.67	-11.22	-16.15
0	2	16	16.07	5.59	4.66	3.08
0	2	17	8.93	5.59	-1.69	-5.33
0	2	18	16.05	8.68	-7.34	4.64
0	2	19	19.21	9.62	6.05	7.48
0	2	20	39.77	13.99	-13.28	-4.39
0	2	21	20.56	6.44	-3.97	-5.07
0	2	22	10.62	0.86	-0.66	0.55
0	2	23	7.75	8.60	-5.01	-6.99
0	2	24	39.11	36.42	34.08	12.84
0	2	25	51.97	40.92	21.92	34.55
0	2	26	65.42	58.83	50.69	-29.86
0	2	27	79.92	70.44	-34.42	-61.46
0	2	28	126.25	108.33	102.86	33.99
0	2	29	79.72	62.32	30.32	54.45
0	2	30	57.16	45.81	39.67	-22.90
0	2	31	36.56	26.32	-13.54	-22.58
0	2	-32	19.17	11.42	10.77	3.80
0	2	-33	9.71	6.89	2.87	6.27
0	2	-34	16.96	13.26	-11.62	6.39
0	2	-35	17.05	11.63	-6.38	-9.72
0	2	-36	17.07	7.41	-6.57	-3.44
0	2	-37	9.82	4.47	-1.17	-4.31
0	2	-38	13.78	12.06	10.32	-6.25
0	2	-39	21.51	18.15	10.20	15.02
0	2	-40	42.23	36.06	33.83	12.50
0	2	-41	31.93	26.51	-13.65	-22.72
0	2	-42	30.98	28.89	25.09	-14.31
0	2	-43	36.58	30.43	14.92	26.52
0	2	-44	52.20	48.57	45.69	16.33
1	1	41	36.75	29.05	-25.00	14.79
1	1	40	24.36	15.55	7.93	13.38
1	1	39	32.75	24.11	-20.83	12.14
1	1	38	43.17	35.62	-17.63	-30.95
1	1	37	24.01	15.95	-13.91	7.80
1	1	36	9.90	5.05	2.57	4.35
1	1	35	9.95	0.94	0.82	-0.45
1	1	34	29.89	17.48	8.91	15.04
1	1	33	22.20	14.39	12.27	-7.52
1	1	32	9.86	6.03	-3.13	-5.16
1	1	31	9.76	1.72	-1.59	0.67
1	1	30	47.15	34.18	-17.02	-29.64
1	1	29	52.73	40.14	-34.87	19.88
1	1	28	39.44	33.74	16.77	29.28
1	1	27	81.43	70.00	-60.59	35.05
1	1	26	137.90	123.34	-62.21	-106.50
1	1	25	67.30	61.73	-53.22	31.27
1	1	24	33.88	26.29	13.31	22.67
1	1	23	32.99	28.28	-24.51	14.11
1	1	22	27.78	23.53	-11.82	-20.35
1	1	21	7.79	2.82	-2.42	1.45
1	1	20	10.70	2.35	-1.36	-1.92
1	1	19	17.98	8.10	6.80	-4.40
1	1	18	27.56	17.17	9.40	14.38
1	1	17	13.79	10.19	8.65	-5.39
1	1	16	9.44	4.87	-2.32	-4.29
1	1	15	6.46	1.46	1.21	-0.82
1	1	14	24.97	24.08	-12.13	-20.80
1	1	13	36.19	38.45	-33.25	19.31
1	1	12	43.96	39.96	20.11	34.53
1	1	11	87.94	101.31	-87.56	50.96
1	1	10	161.09	225.16	-112.82	-194.86
1	1	9	130.43	150.00	-129.94	74.94
1	1	8	96.36	90.92	45.55	78.68
1	1	7	121.02	150.83	-130.55	75.52
1	1	6	157.85	226.59	-113.58	-196.06
1	1	5	86.18	100.23	-86.75	50.21
1	1	4	40.74	36.45	18.17	31.60
1	1	3	24.86	24.77	-21.50	12.31
1	1	2	31.89	18.52	9.27	16.03
1	1	1	52.01	38.22	33.00	-19.28
1	1	0	51.17	32.34	-16.24	-27.97
1	1	-1	72.55	62.66	54.78	-31.30
1	1	-2	112.53	102.85	51.09	89.26
1	1	-3	61.72	46.44	40.24	-23.19
1	1	-4	27.84	14.75	-7.21	-12.87
1	1	-5	7.14	1.87	-1.60	0.97
1	1	-6	60.68	59.88	-29.92	-51.87
1	1	-7	68.79	70.93	-61.59	35.18
1	1	-8	68.33	61.73	30.68	53.57
1	1	-9	118.08	137.55	-119.34	68.41
1	1	-10	169.73	271.01	-135.45	-234.73
1	1	-11	127.28	159.90	-138.58	79.78
1	1	-12	95.49	85.18	42.37	73.89
1	1	-13	111.90	122.04	-105.91	60.64
1	1	-14	129.72	153.56	-76.40	-133.21
1	1	-15	62.38	54.12	-46.88	27.03
1	1	-16	23.64	14.54	7.43	12.50
1	1	-17	8.93	6.56	-5.76	3.14
1	1	-18	13.06	4.59	2.20	4.04
1	1	-19	15.09	6.44	5.79	-2.83
1	1	-20	18.44	4.81	-1.97	-4.39
1	1	-21	20.35	8.97	8.14	-3.77
1	1	-22	29.67	13.59	6.15	12.12
1	1	-23	10.81	3.98	3.59	-1.72
1	1	-24	7.87	2.22	1.33	1.78
1	1	-25	19.84	17.17	-14.83	8.64
1	1	-26	61.73	61.75	-30.49	-53.70
1	1	-27	59.21	55.26	-48.22	27.00
1	1	-28	64.99	39.98	19.66	34.81
1	1	-29	80.25	72.93	-63.30	36.23
1	1	-30	118.17	114.10	-56.88	-98.90
1	1	-31	63.46	50.93	-44.21	25.28
1	1	-32	38.10	18.65	9.26	16.18
1	1	-33	19.35	13.14	-11.39	6.56
1	1	-34	16.97	4.69	1.89	4.30
1	1	-35	19.78	11.47	10.04	-5.53
1	1	-36	17.23	6.87	-3.41	-5.96
1	1	-37	14.09	6.59	5.69	-3.33
1	1	-38	9.94	1.53	-0.95	-1.20
1	1	-39	17.10	8.04	-6.80	4.29
1	1	-40	19.51	8.51	4.45	7.26
1	1	-41	27.13	21.10	-18.27	10.56
1	1	-42	53.04	45.04	-22.49	-39.02
1	1	-43	36.45	28.76	-24.89	14.41
-1	1	9	69.47	73.21	18.74	-70.77
-1	1	8	76.36	64.20	32.24	55.52
-1	1	7	140.76	139.78	-135.09	-35.94
-1	1	6	38.00	31.85	-27.53	16.02
-1	1	5	4.12	1.82	-0.60	1.71
-1	1	4	30.60	17.30	-8.48	-15.08
-1	1	3	119.47	92.43	89.30	23.82
-1	1	2	78.99	56.87	49.12	-28.67
-1	1	1	49.27	30.22	-7.69	29.17
-1	1	0	52.66	29.90	-14.96	-25.88
-1	1	-1	92.69	71.36	68.92	18.51
-1	1	-2	24.15	13.34	11.57	-6.63
-1	1	-3	16.28	9.94	2.54	-9.61
-1	1	-4	45.96	33.76	16.91	29.22
-1	1	-5	174.92	190.93	-184.39	-49.54
-1	1	-6	132.82	133.00	-115.28	66.32
-1	1	-7	77.97	79.97	20.59	-77.28
-1	1	-8	93.57	92.74	46.29	80.36
-1	1	-9	195.65	291.41	-281.45	-75.54
-1	1	-10	112.61	128.20	-110.99	64.16
-1	1	-11	45.99	50.37	13.04	-48.65
-1	1	-12	41.99	37.61	18.87	32.53
-1	1	-13	63.82	71.75	-69.30	-18.59
-1	1	-14	15.29	16.23	-14.12	7.99
-1	1	-15	6.46	1.26	0.13	-1.25
-1	1	-16	6.67	3.17	-1.43	-2.82
-1	1	-17	29.25	18.49	17.69	5.40
-1	1	-18	17.43	10.92	9.69	-5.04
-1	1	-19	10.38	4.93	-1.51	4.69
-1	1	-20	10.70	3.28	-1.51	-2.91
-1	1	-21	11.02	4.34	-4.22	-1.01
-1	1	-22	16.04	15.16	-13.26	7.35
-1	1	-23	18.44	16.37	4.42	-15.76
-1	1	-24	44.82	28.30	13.87	24.67
-1	1	-25	127.70	121.28	-116.86	-32.45
-1	1	-26	79.62	69.28	-60.18	34.33
-1	1	-27	44.60	34.75	9.22	-33.50
-1	1	-28	52.58	32.61	16.23	28.28
-1	1	-29	88.84	76.72	-74.16	-19.66
-1	1	-30	27.22	20.23	-17.42	10.29
-1	1	-31	9.76	1.30	0.15	-1.29
-1	1	-32	13.94	5.40	-2.56	-4.75
-1	1	-33	37.15	26.94	25.89	7.47
-1	1	-34	19.93	11.40	10.03	-5.41
-1	1	-35	9.95	2.08	-0.71	1.96
-1	1	-36	9.90	3.33	1.88	2.75
-1	1	-37	36.68	28.99	-23.12	-7.07
-1	1	-38	33.44	22.04	-19.00	11.16
-1	1	-39	18.91	13.51	3.38	-13.08
2	0	39	24.19	21.49	-15.40	-14.99
2	0	38	21.77	20.18	-0.50	20.17
2	0	37	9.18	6.95	-4.90	4.93
2	0	36	9.43	13.68	13.68	0.39
2	0	35	198.29	176.64	125.89	123.92
2	0	34	176.98	153.16	-0.38	-153.16
2	0	33	93.92	84.71	59.58	-60.21
2	0	32	66.13	65.28	65.28	-0.25
2	0	31	93.26	75.12	53.90	52.33
2	0	30	17.30	8.09	-0.52	8.07
2	0	29	9.95	4.81	-3.59	3.20
2	0	28	13.96	10.65	10.65	-0.23
2	0	27	96.24	90.24	63.57	64.04
2	0	26	59.47	55.73	0.55	-55.72
2	0	25	23.28	13.71	9.89	-9.48
2	0	24	39.66	31.77	-31.77	0.43
2	0	23	321.62	330.45	-235.17	-232.14
2	0	22	232.93	253.34	1.10	253.34
2	0	21	140.47	116.26	-81.98	82.44
2	0	20	48.79	42.53	-42.53	-0.15
2	0	19	203.28	235.57	166.88	166.26
2	0	18	220.38	259.06	-0.63	-259.06
2	0	17	145.81	149.72	105.59	-106.14
2	0	16	152.67	131.30	131.30	-0.11
2	0	15	198.73	222.68	158.25	156.66
2	0	14	23.71	8.11	-0.07	8.11
2	0	13	48.56	46.69	-33.13	32.89
2	0	12	47.43	41.29	-41.29	-0.04
2	0	11	119.77	107.66	76.05	76.20
2	0	10	182.58	207.78	-0.55	-207.78
2	0	9	129.67	134.71	95.26	-95.25
2	0	8	117.84	96.09	96.09	0.33
2	0	7	6.40	1.83	1.27	1.32
2	0	6	139.18	128.65	0.12	128.65
2	0	5	95.56	90.99	-64.20	64.48
2	0	4	120.28	92.82	-92.82	0.19
2	0	3	218.83	193.38	-136.78	-136.70
2	0	2	20.44	5.87	0.21	-5.86
2	0	1	79.63	64.75	45.69	-45.88
2	0	0	124.73	106.28	106.28	-0.34
2	0	-1	243.36	274.15	193.45	194.26
2	0	-2	67.66	61.16	-0.52	-61.16
2	0	-3	24.34	24.06	17.28	-16.74
2	0	-4	74.97	65.76	65.75	0.53
2	0	-5	286.42	348.65	246.56	246.50
2	0	-6	182.54	155.71	0.13	-155.71
2	0	-7	28.81	24.51	17.19	-17.47
2	0	-8	50.86	40.48	-40.48	-0.08
2	0	-9	270.71	281.13	-198.32	-199.26
2	0	-10	192.37	176.63	-0.33	176.63
2	0	-11	113.62	79.28	-56.00	56.12
2	0	-12	36.00	29.51	-29.51	0.16
2	0	-13	227.58	221.26	156.92	155.98
2	0	-14	242.82	245.15	1.11	-245.14
2	0	-15	142.88	124.83	87.86	-88.68
2	0	-16	92.53	64.15	64.15	-0.61
2	0	-17	99.62	75.56	-53.45	-53.41
2	0	-18	129.99	97.15	0.72	97.15
2	0	-19	33.28	22.31	-15.95	15.59
2	0	-20	43.11	42.73	42.73	-0.60
2	0	-21	329.93	371.26	261.12	263.91
2	0	-22	250.58	274.95	0.18	-274.95
2	0	-23	148.19	145.96	103.62	-102.80
2	0	-24	133.46	103.16	103.16	0.27
2	0	-25	24.23	16.64	-11.83	-11.70
2	0	-26	186.97	186.93	-1.40	186.92
2	0	-27	144.74	133.73	-94.58	94.54
2	0	-28	162.43	119.51	-119.51	-0.12
2	0	-29	184.28	177.93	-124.06	-127.55
2	0	-30	9.46	5.29	-1.63	-5.04
2	0	-31	25.41	26.45	18.70	-18.71
2	0	-32	47.69	29.69	29.68	0.75
2	0	-33	55.68	58.25	41.26	41.12
2	0	-34	9.93	1.24	1.23	0.20
2	0	-35	9.98	7.07	-4.95	5.06
2	0	-36	24.49	10.32	10.32	0.28
2	0	-37	171.17	171.34	120.39	121.91
2	0	-38	153.78	153.58	1.58	-153.57
2	0	-39	74.19	84.51	59.65	-59.86
2	0	-40	81.02	66.28	66.28	-0.34
2	0	-41	74.16	84.33	58.71	60.54
2	0	-42	9.26	5.45	0.61	5.42
2	0	-43	12.70	10.37	-7.29	7.37
2	0	-44	12.25	8.00	-7.99	-0.47
2	0	-45	11.73	9.60	-6.24	-7.29
2	0	-46	11.15	1.29	-1.19	0.49
2	0	-47	7.43	4.92	-3.81	3.12

The $02\hat{L}$ reflections show an intensity distribution approximately equal to $\sqrt{7}$, $\sqrt{3}$, $\sqrt{3}$, $\sqrt{3}$ for $\hat{L}=0$, 1, 2, and 3. Two polytypes have this distribution – the $4Tc_3$ and $4Tc_5$ models. However, the $11\hat{L}$ and $\bar{1}1\hat{L}$ observed and calculated intensities agree only for the $4Tc_5$ form (Table 3).

In order to verify this method of determining the stacking sequence, structure factors of the five possible models were calculated for 284 reflections ($00L$, $02L$, $11L$, $\bar{1}1L$, and $20L$) using the structure factor program in 'X-ray System 63' (Stewart & High, 1964). The atomic coordinates and isotropic temperature factors for 80 atoms in the asymmetric unit were derived from those of the $1M$ lithium fluormica structure (Takeda & Donnay, 1966) using the (PLYTP) FORTRAN program. By adjusting only the scale factors, the R index for $4Tc_5$ is 18%. The other four models gave R's of over 30%. The atomic coordinates and temperature factors for the $4Tc_5$ structure are given in Table 4. The observed and calculated structure factors for the $4Tc_5$ structure are given in Table 5.

Discussion

The $4Tc_5$ polytype described here has a stacking sequence in which the *relative* layer rotations are 0, 60, 180, and 120° (Ross, Takeda & Wones, 1966). The vector stacking symbol for this polytype is $4Tc_5[0132]$; the Zvyagin symbol is $\bar{C}\bar{C}\bar{A}A$. This is of mineralogical interest since this is only the second mica polytype so far identified that contains relative layer rotations other than 0 and ±120°. The common lithium bearing mica, lepidolite, often has a $2M_2$ structure in which relative layer rotations of ±60° occur. The $1M$ lithium fluormica structure shows little ditrigonality of the basal oxygen layers (tetrahedral rotation, $\alpha=6°13'$, Takeda & Donnay, 1966); thus relative layer rotations of ±60 and 180° may be permissible in micas having this composition (Radoslovich, 1958). Non-lithium bearing micas are generally expected to have tetrahedral rotations of 10° or more. In such structures the ditrigonal nature of the basal oxygen layer is so strong that probably only relative layer rotations of 0 and ±120° are possible.

Polytypism in micas has often been confused with twinning. Because of the very symmetrical nature of the mica structure, twinning produces a metrically hexagonal lattice which has a c dimension three times larger than that of the true unit cell. Therefore, a polytype that has an apparent layer repeat of $N=3n$, where n is any integer, could be interpreted as a twin of a simpler polytype with the layer repeat of $N/3$, particularly if the volumes of the various twin units are equal or nearly equal (Sadanaga & Takéuchi, 1961). Smith & Yoder (1956) previously pointed out the similarity of the single-crystal X-ray patterns of the twinned $1M$ polytype to those of the $3T$ mica. The diffraction patterns of the $4Tc_5$ polytype described here cannot be interpreted as due to twinning, for the layer repeat is not divisible by three.

Extinctions, other than space-group extinctions, sometimes called 'structural extinctions' or 'additional extinctions' provide a method of determining the stacking sequences of the simpler mica polytypes as pointed out by Ross, Takeda & Wones (1966). However, for more complicated mica forms, particularly those with layer repeats greater than four, the characteristic 'periodic intensity distribution' must be analyzed in order to be sure of the correct stacking sequence. It should be noted that 'additional extinctions' are a part of information of the periodic intensity distribution function. More than one polytype may give the same 'additional extinctions'.

The determination of the stacking sequence of mica polytypes by regular methods of structural analysis, such as Patterson syntheses and direct phase determinations, requires that large amounts of data be collected and processed. The method described in this paper provides a quick and accurate method of determining stacking sequences of mica polytypes. Even rough visual estimates of intensities using a strong, medium, weak and extinct classification can distinguish the correct model when the $\overline{S_c^N}(hk\hat{L})$ values for each possible model have been generated. In future publications we will describe a number of new mica polytypes that were identified by this procedure.

The intensity distribution function given in this paper can be applied to other types of crystal structure, for example, tridymite-cristobalite, talc, pyrophyllite, the kaolin minerals, as well as SiC, CdI_2, and ZnS.

I wish to thank Dr Hatten S. Yoder, Jr. (Geophysical Laboratory, Carnegie Institution, Washington, D.C.) for providing the lithium fluormica sample. The majority of the computations were performed at the Computer Science Center, The University of Maryland, through the courtesy of Professor J. M. Stewart (Department of Chemistry, The University of Maryland).

The author also thanks Professor J. D. H. Donnay for the interest given him during the course of this work, which in part was carried out under NSF grant GP 1565 at the Crystallographic Laboratory, The Johns Hopkins University. This study was completed at the U.S. Geological Survey, where the author was a guest investigator in 1965. He is indebted to Dr Malcolm Ross and Dr David R. Wones (U.S. Geological Survey) for their collaboration in studies of the mica polytypes and for assistance in the preparation of the manuscript.

References

Burnham, C. W. & Radoslovich, E. W. (1964). *Carnegie Institution of Washington Yearbook*, **63**, 232.

Busing, W. R., Martin, K. O. & Levy, H. A. (1962). *ORFLS, A FORTRAN Crystallographic Least-Squares Program.* Oak Ridge National Laboratory, Tennessee, report ORNL-TM-305.

HEINRICH, E. W., LEVINSON, A. A., LEVANDOWSKI, D. W. & HEWITT, C. H. (1953). *Studies in the Natural History of Micas, September* 1951-*August* 1953. Univ. of Michigan Engineering Research Institute Project M978, Final Report, 241 pp.
HENDRICKS, S. B. & JEFFERSON, M. E. (1939). *Amer. Min.* **24**, 729.
LIPSON, H. & TAYLOR, C. A. (1958). *Fourier Transforms and X-Ray Diffraction*. London: Bell.
RADOSLOVICH, E. W. (1958). *Nature, Lond.* **183**, 253.
ROSS, M., TAKEDA, H. & WONES, D. R. (1966). *Science*, **151**, 191.
ROSS, M. & WONES, D. R. (1965). *Amer. Min.* **50**, 291.
SADANAGA, R. & TAKÉUCHI, Y. (1961). *Z. Kristallogr.* **116**, 406.
SADANAGA, R. & TAKEDA, H. (1964). *Mineral. J. (Japan)*, **4**, 159.
SMITH, J. V. & YODER, H. S., JR. (1956). *Miner. Mag.* **31**, 209.
STEWART, J. M. & HIGH, D. (1964). '*X-ray* 63' *Program System for X-ray Crystallography*. Unpublished program system of the Univ. of Maryland, College Park, Maryland.
TAKEDA, H. (1961). Doctoral dissertation, Univ. Tokyo, Tokyo, Japan.
TAKEDA, H. & DONNAY, J. D. H. (1965). A.C.A. Program and Abstracts, Winter Meeting, Suffern, N.Y., 23.
TAKEDA, H. & DONNAY, J. D. H. (1966). *Acta Cryst.* **20**, 638.
ZVYAGIN, B. B. (1961). *Kristallografiya*, **6**, 714. Also in *Soviet Phys. Crystallogr.* **6**, 571 (Eng. trans.).

Acta Cryst. (1967). **22**, 853

The Crystal Structure of Bis(diethyldithiophosphato)nickel(II), Ni $[(C_2H_5O)_2PS_2]_2$

BY J. F. MCCONNELL AND V. KASTALSKY

School of Physics, University of New South Wales, Sydney, Australia

(*Received* 1 *August* 1966)

Bis(diethyldithiophosphato)nickel(II) is monoclinic, space group $P2_1/c$, with two molecules per unit cell. Unit-cell dimensions, determined with the use of standardized silicon powder and computed by the method of least-squares, are $a=10\cdot493\pm0\cdot005$, $b=10\cdot300\pm0\cdot003$, $c=8\cdot76\pm0\cdot01$ Å, $\beta=102\cdot59\pm0\cdot05$°.

The structure has been determined from a three-dimensional Patterson synthesis and a series of three-dimensional Fourier syntheses. Refinement was by the method of full-matrix least-squares, using data of the type $h0l-h7l$, to the final residual of 0·115. The molecule itself is centrosymmetric with nickel at the centre of symmetry. The nickel and four sulphur atoms are in square planar configuration, with nickel–sulphur bonds of 2·23 and 2·24 Å, which are well within the range 2·1–2·3 Å found for other square planar nickel(II) complexes. The nickel atom shows no tendency to coordinate to any atom in other molecules.

Introduction

This diamagnetic compound was first prepared by Malatesta & Pizzotti (1945) and since then consideration has been given to its probable molecular structural formula together with the structural formulae of similar complexes. Quite recently Lopez-Castro & Truter (1963) observed that in diamagnetic nickel(II) complexes the Ni–S distance is 2·1–2·3 Å, whereas in six-coordinate complexes it is 2·4–2·6 Å. They have commented that this is in accordance with ligand-field theory which predicts that the stronger field produced by the ligands closer to the nickel will cause the d_γ electrons to pair in the d_{z^2} orbitals, so producing a diamagnetic complex with no close neighbours in the z direction. Hence the most likely structural configuration for this compound would be one shown in Fig. 1(*a*) with a nickel atom and four sulphur atoms in square planar configuration. Other configurations, shown in Fig. 1(*b*), (*c*) and (*d*), were considered possible but less likely.

This compound has, however, a few rather unusual properties:

(i) Four-membered rings like Ni–S–P–S in Fig. 1(*a*) are comparatively rare. When this investigation was commenced, only one such structure was fully determined (Barclay & Hoskins, 1962) but since then another similar structure (Franzini, 1963) has been reported.

(ii) Its deep purple colour is unusual, as most diamagnetic square-planar nickel compounds are yellow, brown or red.

(iii) It has a high solubility in most solvents including non-polar light petroleum.

These properties have raised doubts about the correctness of the theoretical predictions, and an investigation of its structure by X-ray methods was undertaken in order to resolve any uncertainties.

Since the completion of the structure determination we have learned of a preliminary communication regarding $Ni[(OEt)_2PS_2]_2$ by Glinskaya & Porai-Koshits (1959) which gave a space group, a unit cell, and the Ni–S distance and configuration in good agreement